Concluding Remarks. The ESR study described here provides evidence for ethylene extrusion reaction 5b and its analogues previously observed in the gas phase.[14] In addition, the structure of the dimer radical cation has been characterized. This σ^* species plays an important role as a high-energy intermediate along the reaction path leading to ethylene extrusion. The use of an MO correlation diagram further clarifies the fine details of this reaction, the driving force being attributed to a transfer of the unpaired electron from the σ^* orbital to the vacating p orbital on sulfur as the ethylene molecule is eliminated in a concerted manner.

Acknowledgment. Our thanks go to Professor Stephen F. Nelsen for permission to refer to his unpublished calculations on the ring-closed oxirane and oxetane cations and to Professor Ben Freiser for a most useful discussion. This research has been supported by the Division of Chemical Sciences, U.S. Department of Energy (Report No. DOE/ER/02968-166).

Registry No. Thietane, 287-27-4; thiirane, 420-12-2; thiirane radical cation, 76095-25-5; thrietane radical cation, 22026-38-6; dimethyl sulfide cation, 34480-65-4; 1,1-dithiirane radical cation, 110372-91-3; 1,1-dithietane radical cation, 66851-53-4; bis(dimethyl sulfide) radical cation, 51137-15-6; 2-thietanyl radical, 110372-92-4; methylthiomethyl radical, 31533-72-9; $CF_3CCl_2CH_2CH_2^{\bullet}$, 110372-93-5; $CF_2ClCFClCH_2CH_2^{\bullet}$, 110372-94-6.

(57) (a) Russell, G. A.; Danen, W. C. *J. Am. Chem. Soc.* **1966**, *88*, 5663; **1968**, *90*, 347. (b) Kornblum, N.; Michel, R. E.; Kerber, R. C. *J. Am. Chem. Soc.* **1966**, *88*, 5662. (c) Bunnett, J. F. *Acc. Chem. Res.* **1978**, *11*, 413.

A Simple Model for the Kinetics of Dissociative Electron Transfer in Polar Solvents. Application to the Homogeneous and Heterogeneous Reduction of Alkyl Halides

Jean-Michel Savéant

Contribution of the Laboratoire d'Electrochimie Moléculaire de l'Universite de Paris 7, Unité Associée au CNRS No. 438, 2 Place Jussieu, 75251 Paris, Cedex 05, France.
Received March 12, 1987

Abstract: A simple model describing the kinetics of electron transfer–bond breaking concerted reactions is developed. On the basis of a Morse curve description of the potential energy surfaces for bond breaking, it leads, for homogeneous and heterogeneous processes, to a quadratic activation-driving force free energy relationship with a standard activation free energy being the sum of two contributions characterizing bond breaking and solvent reorganization, respectively. The latter factor can be estimated on the basis of the Marcus dielectric continuum model. The bond-breaking contribution appears as equal to one-fourth of the bond dissociation energy. Application to the electrochemical and homogeneous reduction of alkyl halides shows a satisfactory agreement between the experimental data and the predictions of the theory. The bond-breaking contribution is typically 80% of the total, the remaining 20% concerning solvent reorganization.

Theoretical models of the kinetics of electron transfer in the liquid phase and attempts to test their predictions experimentally have so far dealt with reactions in which both members of the redox couple are chemically stable, not involving the breaking or formation of bonds, within the time scale of the experiment. In this context, the theory developed by Marcus and others[1] leads to a quadratic driving force–free energy relationship

$$\Delta G_1^{\ddagger} = \Delta G_0^{\ddagger}\left(1 + \frac{\Delta G^\circ}{4\Delta G_0^{\ddagger}}\right)^2 \qquad (1)$$

for both homogeneous and heterogeneous (electrochemical) electron transfers ($\Delta G_1^{\ddagger}$, free energy of activation for the forward reaction; ΔG°, standard free energy of the reaction, $-\Delta G^\circ$ being a measure of the driving force of the reaction). The standard free energy of activation, $\Delta G_0^{\ddagger}$, i.e., the free energy of activation at zero driving force, appears as the sum of two factors featuring the reorganization of the nucleii configuration accompanying electron transfer. One, the external reorganization factor, concerns the fluctuational reorganization of the solvent molecules. It can be expressed as a function of the reactant radii and of the optical and static dielectric constants of the solvent in the framework of a hard-sphere Born model of solvation. The other, the internal reorganization factor, features the changes in bond lengths and angles accompanying electron transfer. It can be expressed as a function of the net variation in bond lengths and angles and of the corresponding force constants in the reactants and products. The theoretical predictions appear to be in fair agreement with the experimental observations both as regards the quadratic form of the activation driving force free energy relationship (1)[2] and the magnitude of the activation free energies in terms of internal[1d] and external[3] reorganization factors.

Recent investigations of the electrochemical reduction of aliphatic halides and of their homogeneous reduction by redox reagents[4] has provided a typical example of dissociative electron transfer, i.e., a reaction in which the transfer of the electron and the breaking of a bond are concerted processes.[5] The kinetics

(1) (a) Marcus, R. A. *Annu. Rev. Phys. Chem.* **1964**, *15*, 155. (b) Marcus, R. A. *J. Chem. Phys.* **1965**, *43*, 679. (c) Waisman, E.; Worry, G.; Marcus, R. A. *J. Electroanal. Chem.* **1977**, *82*, 9. (d) Marcus, R. A. *Faraday Discuss. Chem. Soc.* **1982**, *74*, 7. (e) Marcus, R. A.; Sutin, N. *Biochim. Biophys. Acta* **1985**, *811*, 265.

(2) Savéant, J. M.; Tessier, D. *Faraday Discuss. Chem. Soc.* **1982**, *74*, 57 and references cited therein.

(3) (a) Peover, M. E.; Powell, J. S. *J. Electroanal. Chem.* **1969**, *20*, 427. (b) Kojima, H.; Bard, A. J. *J. Am. Chem. Soc.* **1975**, *97*, 6317. (c) Fawcett, W. R.; Jaworski, J. S. *J. Phys. Chem.* **1983**, *87*, 2972. (d) Jaenicke, W. *J. Chem. Soc., Faraday Trans. 1* **1987**, *83*, 161. (e) As revealed by a systematic study of homogeneous and heterogeneous electron transfer in a large series of aromatic compounds in an aprotic dipolar solvent, dimethylformamide,[3b] the solvent reorganization factor appears smaller than predicted by the theory. This point is discussed in more details further on.

(4) (a) I.e., that are able to transfer an electron without the transient formation of an adduct with the substrate.[4b,c] (b) Andrieux, C. P.; Dumas-Bouchiat, J. M.; Savéant, J. M. *J. Electroanal. Chem.* **1978**, *87*, 39. (c) Lexa, D.; Saveant, J. M.; Su, K. B.; Wang, D. L. *J. Am. Chem. Soc.*, in press.

(5) (a) Andrieux, C. P.; Merz, A.; Saveant, J. M.; Tomahogh, R. *J. Am. Chem. Soc.* **1984**, *106*, 1957. (b) Andrieux, C. P.; Merz, A.; Savéant, J. M. *J. Am. Chem. Soc.* **1985**, *107*, 6097. (c) Andrieux, C. P.; Gallardo, I.; Saveant, J. M.; Su, K. B. *J. Am. Chem. Soc.* **1986**, *108*, 638. (d) Andrieux, C. P.; Savéant, J. M.; Su, K. B. *J. Phys. Chem.* **1986**, *90*, 3815.

0002-7863/87/1509-6788$01.50/0

of the heterogeneous and homogeneous reactions were analyzed in terms of Marcus quadratic activation–driving force free energy relationship.[5b-d] This approach, however, suffers from two drawbacks deriving from the fact that Marcus theory is not devised for dissociative electron transfer. One is that it is not certain that the quadratic activation–driving force relationship depicted by eq 1 is correct for dissociative electron transfers.[6] The other is that the dependence of the standard activation free energy, $\Delta G_0^{\ddagger}$, upon reorganization factors, particularly upon the strength of the carbon–halogen bond,[7] is not known.

On the other hand, although systematic kinetic studies of experimental examples have been much less developed than for electron transfer reactions not involving bond breaking, dissociative electron transfer is likely to occur in the reduction or oxidation of a large number of molecules in which the electrophore contains a frangible σ-bond. This not only concerns organic compounds but also coordination complexes and small inorganic molecules.[8]

We describe in the following a simple model of the kinetics of dissociative electron transfer in polar solvents showing the validity of the quadratic activation–driving force free energy relationship depicted by eq 1 and relating the standard activation free energy to the bond dissociation energy as well as to the solvent reorganization. The homogeneous and heterogeneous reduction of alkyl halides in organic aprotic solvents will be taken as an example for testing the validity of the model.

Results and Discussion

Description of the Model. The reaction is noted:

$$R\text{–}X + e^- \rightarrow R^\bullet + X^- \qquad \text{(electrochemical)}$$

$$R\text{–}X + A^{\bullet -} \rightarrow R^\bullet + X^- + A \qquad \text{(homogeneous)}$$

R–X stands not only for alkyl halides but also for any molecule, X designing the "leaving group", i.e., the group which leaves carrying on an electron pair and R the "remaining group", i.e., the group remaining with an unpaired electron. $A/A^{\bullet -}$ is a chemically stable redox couple reacting in an outer-sphere manner, as does the electrode in the first case, in the sense that it is assumed that there is no formation of adduct between the members of this couple and the substrate or intermediates of the reduction of RX.

The model is based on the following assumptions and approximations.

The Born–Hoppenheimer approximation is assumed to hold and the reaction to be adiabatic.

The potential energy surfaces for the reactants and products depend upon two types of nuclear coordinates describing the solvent fluctuational configuration on one hand and the R–X distance on the other. The two reorganization free energies are regarded as independent one from the other, i.e., the total reorganization free energy is the sum of two independent terms. For simplicity, the contribution of other vibration modes, besides R–X stretching, is omitted. The theory can, however, be easily extended to include this contribution if necessary.

The potential energy of the reactants is assumed to depend upon the R–X distance according to the RX Morse curve

$$U_R = D_{RX}[1 + \exp(-2\beta y) - 2\exp(-\beta y)]$$

(y is the R–X distance minus the equilibrium bond distance in the reactant. The potential energy is zero at the minimum of the Morse curve. D_{RX} is the dissociation energy of the R–X bond, $\beta = \nu_0(2\pi^2\mu/D_{RX})^{1/2}$ with ν_0 representing the vibration frequency of the RX bond and μ the reduced mass of the C and X atoms.)

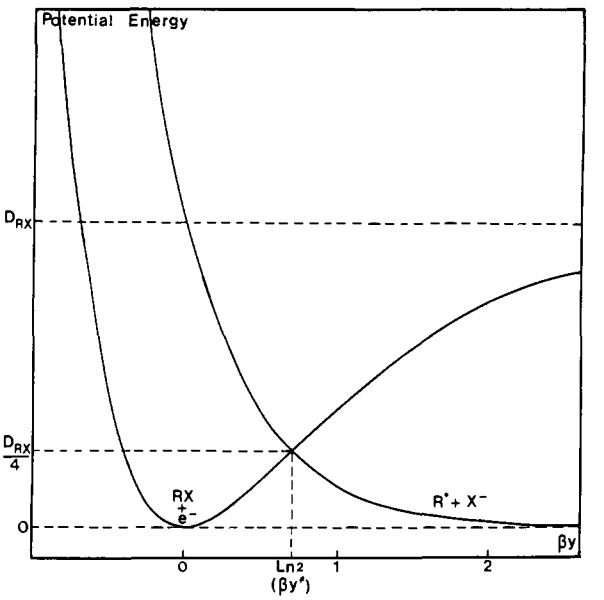

Figure 1. Morse curves for the reactants and products at zero driving force (y, elongation of the R–X distance from equilibrium; $\beta = \nu_0(2\pi^2\mu/D_{RX})^{1/2}$; ν_0, vibration frequency; μ, C and X, reduced mass; D_{RX}, bond dissociation energy).

The next important approximation is that for the products, $R^\bullet + X^-$, the potential energy surface is assumed to be the repulsive part of the *reactant* Morse curve, i.e., $\exp(-2\beta y)$. The assumption that the repulsive part of the $R^\bullet + X^-$ (reactants) and $R^\bullet + X^-$ (products) is the same has previously been made in the interpretation of the kinetics of gas-phase thermal electron attachment to alkyl halides.[9] This was based on the fact that the repulsive term arises from interactions with the core electrons and nucleii which should not be significantly altered by the presence of a single peripheral electron.[9] In addition to that, we neglect here the possible attractive interactions between $R^\bullet$ and X^-. These are likely to result from induced dipole-charge and quadrupole-charge interactions. We assumed that these are small, smaller than in the gas phase, owing to the presence of a surrounding polar medium.[10] The reactant and product potential energy curves are shown in Figure 1.

The solvent fluctuational reorganization is treated according to the Marcus dielectric continuum model,[1b,c] leading to a quadratic expression of the Gibbs free energy

$$\Delta G = \frac{\kappa}{2}(x - x_1)^2$$

for the reactants and

$$\Delta G = \frac{\kappa}{2}(x - x_2)^2$$

for the products, where κ is the corresponding force constant and x a fictitious charge serving as a coordinate that represents the fluctuational configuration of the solvent (x_1 and x_2 are the values of the fictitious charge for the reactants and products, respectively). This assumes that the force constant, κ, for the solvent reorganization is the same for RX and $R^\bullet + X^-$ in the region where the two $U(y)$ curves cross. This is a reasonable assumption in view of the fact that the $R^\bullet$,X^- distance is not very different from the R–X equilibrium distance at the transition state.[11]

(6) (a) Although it is likely that the potential energy surfaces for a large number of reactions, possibly involving bond breaking and/or bond formation, could lead to the same quadratic form of the activation-driving force relationship.[6b-g] (b) Magnoli, D. E.; Murdoch, J. R. *J. Am. Chem. Soc.* **1986**, *103*, 7465. (c) Murdoch, J. R.; Magnoli, D. E. *J. Am. Chem. Soc.* **1982**, *104*, 3792. (d) Murdoch, J. R. *J. Am. Chem. Soc.* **1983**, *105*, 2159. (e) Murdoch, J. R. *J. Am. Chem. Soc.* **1983**, *105*, 2667. (f) Kurz, J. G. *Chem. Phys. Lett.* **1978**, *57*, 243. (g) Grunwald, E. *J. Am. Chem. Soc.* **1985**, *107*, 125.

(7) Qualitatively, $\Delta G_0^{\ddagger}$ appears to be an increasing function of the strength of the carbon–halogen bonds.[5d]

(8) (a) Coordination complexes in which the coordination number changes with the oxidation state as, e.g., in the case of the cobalt(II)/cobalt(I) couple in vitamin B12 derivatives.[8b] Inorganic molecules such as, for example, hydrogen peroxide. (b) Lexa, D.; Savéant, J. M. *Acc. Chem. Res.* **1983**, *16*, 235.

(9) Wentworth, W. E.; George, R.; Keith, H. *J. Chem. Phys.* **1969**, *51*, 1791.

(10) The presence of a supporting electrolyte further tends to decrease the energy of such interactions.

(11) As will be seen below, the elongation of the R–X bond in the transition state ranges from 0.22 to 0.35 Å for, e.g., butyl halides.

Lastly, it is assumed, for the sake of simplicity, that the reorganization factor characterizing the $A/A^{\bullet-}$ couple involves solvent reorganization only.[12]

Under these conditions, the free energies are expressed as[13]

$$G_R = G^\circ_R + D_{RX}[1 + \exp(-2\beta y) - 2\exp(-\beta y)] + \frac{\kappa}{2}(x - x_1)^2 \quad (2)$$

for the reactants and

$$G_P = G^\circ_P + D_{RX}\exp(-2\beta y) + \frac{\kappa}{2}(x - x_2)^2 \quad (3)$$

for the products.

It follows (for a detailed derivation of the following relationships see the Appendix) that the activation–driving force relationship has a quadratic form[14,15]

$$\Delta G_1^\ddagger = \Delta G_0^\ddagger\left(1 + \frac{\Delta G^\circ}{4\Delta G_0^\ddagger}\right)^2 \quad (1)$$

$$\Delta G_{-1}^\ddagger = \Delta G_0^\ddagger\left(1 - \frac{\Delta G^\circ}{4\Delta G_0^\ddagger}\right)^2 \quad (4)$$

with the standard activation free energy being given by

$$\Delta G_0^\ddagger = \frac{D_{RX}}{4} + \frac{\lambda_0}{4} \quad (5)$$

with $\lambda_0 = (\kappa/2)(x_1 - x_2)^2$ being the usual Marcus–Hush[1b,c,16] solvent reorganization factor.

We thus end up with a quite simple estimation of the contribution of bond breaking to the standard activation free energy: one fourth of the bond energy.

In gas-phase studies of similar reactions,[9] the repulsive part of the $R^\bullet + X^-$ potential energy curve was considered as being the same as that of RX. However, the attractive part was not neglected, as we did above, but was assumed to be the product of the attractive part of the RX curve and an empirical parameter γ. Treatment of the gas-phase experimental data by the resulting potential energy curves led to values of γ ranging from 0.1 to 0.3. Using the same model here, i.e., taking as expressions of the free energy of the reactants and products

$$G_R = G^\circ_R + D_{RX}[1 + \exp(-2\beta y) - 2\exp(-\beta y)] + \frac{\kappa}{2}(x - x_1)^2 \quad (6)$$

i.e., $$G_R = G^\circ_R + D_{RX}[1 - \exp(-\beta y)]^2 + \frac{\kappa}{2}(x - x_1)^2$$

$G_P =$

$$G^\circ_P + D_{RX}[\exp(-2\beta y) - 2\gamma\exp(-\beta y) + \gamma^2] + \frac{\kappa}{2}(x - x_2)^2 \quad (7)$$

i.e., $$G_P = G^\circ_P + D_{RX}(\gamma - \exp(-\beta y)]^2 + \frac{\kappa}{2}(x - x_2)^2$$

the following rate law ensues (see Appendix for details on its derivation).

Equations 1 and 4 still apply, but now with

$$\Delta G_0^\ddagger = \tfrac{1}{4}[(1 - \gamma)^2 D_{RX} + \lambda_0] \quad (8)$$

Note that the product potential energy curve exhibits a minimum for $y = -(\ln\gamma)/\beta$ corresponding to an energy $-D_{RX}\gamma^2$ as compared to the energy of the state where $R^\bullet$ and X^- are infinitely distant. The energy of this minimum is taken as reference of the driving force in the above derivation. Note also that, since γ is small (see below), this is a shallow minimum where the $R^\bullet,X^-$ distance is much larger than bonding distances which falls in line with the concept of a weak charge/induced dipole interaction between X^- and $R^\bullet$

Application to the Homogeneous and Heterogeneous Reduction of Alkyl Halides in Aprotic Solvents. We now test the two models described above using the electrochemical and redox catalysis data previously obtained for the reduction of *n*-, *sec*-, and *tert*-butyl iodides, bromides, and chlorides.[5c,d] Testing the models requires the knowledge of a series of characteristic quantities that are listed in Table I.

Estimation of the standard potentials of the $RX/R^\bullet + X^-$ couple, $E^\circ_{RX/R^\bullet+X^-}$, was made as already described,[5c] using the method first introduced by Hush[17a] and further developed by Eberson,[17b]

$$E^{\circ DMF,aq.SCE}_{RX/R^\bullet+X^-} = \Delta G^{\circ g}_{f,RX} - \Delta G^{\circ g}_{f,R^\bullet} - \Delta G^{\circ DMF}_{f,X^-} - \Delta G^\circ_4 - 0.183$$

in volts, the free energies being expressed in eV. The three ΔG°_f are the standard free energies of formation from the elements and ΔG°_4 the free energy of the reaction

$$RX^{DMF} + R^{\bullet g} \rightleftarrows RX^g + R^{\bullet DMF}$$

The estimation of ΔG°_4 deserves further attention. Thus far[5c,17a,b] it was based on the following assumptions and approximations.[17a,b] ΔG°_4 is the same in water and in DMF. It is the same whatever R and taken equal to its value for $R = CH_3$. $CH_3^\bullet$ is assumed to have the same free energy of solvation as CH_4.[17a] The latter appears in fact not quite correct in view of the likely interactions between the solvent dipoles and $R^\bullet$ regarded as a quadrupole and an induced dipole. The truth is thus probably between the value of ΔG°_4 estimated as described above and $\Delta G^\circ_4 = 0$. We estimated $E^\circ_{RX/R^\bullet+X^-}$ as being bracketed by these two values (Table I) and tested the models using successively the two values.

The C–X bond dissociation energies, D_{RX}, were estimated from thermochemical tables[18] and the factor β in the Morse curves from

(12) If necessary, the analysis could be extended without major difficulty to the case where internal $A/A^{\bullet-}$ reorganization contributes significantly.

(13) Since the vibrations along the R–X bond and the $R^\bullet + X^-$ approach are treated classically, the distribution function, ρ, tends toward zero and thus in the expression of the free energy[1c] $\Delta F = \int \rho U\, dq + kT\int \rho \ln \rho\, dq$ (q = set of nuclear coordinates), the second term vanishes as is the case in the treatment of harmonic vibrations for electron transfers without bond breaking.[1b]

(14) The relationship is even "more quadratic" than the Marcus relationship in the sense that it is strictly quadratic in the presence case whereas it is approximately quadratic Marcus theory as a result of neglecting the antisymmetric component of the reactant and product force constants.[1b]

(15) (a) ΔG° is the standard Gibbs free energy of the reaction taking as initial and final states the precursor and successor complexes, respectively, i.e., taking into account the work terms required for bringing the reactants and products from infinite distance to contact.[1b,c] In the electrochemical case, introduction of the work terms amounts to correcting the apparent rate constant from the double layer effects.[5b] (b) Delahay, P. *Double Layer and Electrochemical Kinetics*; Interscience: New York, 1965.

(16) (a) For the cross-exchange reaction between RX and $A^{\bullet-}$[1b]

$$\lambda_0^{hom} = e_0^2\left(\frac{1}{D_{op}} - \frac{1}{D_S}\right)\left(\frac{1}{2a_1} + \frac{1}{2a_2} - \frac{1}{d}\right)$$

where e_0 is the charge of the electron, D_{op} and D_S are the optical and static dielectric constants of the solvent, respectively, a_1 and a_2 are the radii of the spheres equivalent to the RX and A molecules, and d is the distance of their center in the precursor complex, in practice the sum of their radii. In the electrochemical case

$$\lambda_0^{het} = e_0^2\left(\frac{1}{D_{op}} - \frac{1}{D_S}\right)\frac{1}{4a_1}$$

in Marcus theory which takes into account the image forces[1b] and

$$\lambda_0^{het} = e_0^2\left(\frac{1}{D_{op}} - \frac{1}{D_S}\right)\frac{1}{2a_1}$$

in Hush theory[15h] which neglects the effect of image forces. (b) Hush, N. S. *J. Chem. Phys.* **1958**, *28*, 962.

(17) (a) Hush, N. S. *Z. Elektrochem.* **1957**, *61*, 734. (b) Eberson, L. *Acta Chem. Scand. Sect. B* **1982**, *B36*, 533.

(18) Benson, S. W. *Thermodynamical Kinetics*, 2nd ed.; Wiley: New York, 1976.

(19) (a) Bellamy, L. J. *The Infrared Spectra of Complex Molecules*; Chapman and Hall: London, 1975; p 368. (b) *Handbook of Chemistry and Physics*; 52nd ed.; The Chemical Rubber Co.: Cleveland, 1971; p F173. (c) *Ibid.*, p D146.

Table I. Characteristic Quantities for Butyl Halides

compd	$E^\circ_{RX/R\cdot+X^-}$[a] $\Delta G^\circ_4 = 0$	$E^\circ_{RX/R\cdot+X^-}$[a] $\Delta G^\circ_4 \neq 0$[b]	a_1[c] (Å)	λ_0^{hom}[d] (eV)	λ_0^{het}[d] (eV)	D_{RX}[e] (eV)	β[f] (Å^{-1})	$y^\ddagger$[g] (Å)	C-X dist (Å) ‡[h]	C-X dist (Å) VVC[i]
n-BuI	−1.075	−1.209	2.88	0.633	0.723	2.56	1.57	0.44	2.57	4.00
sec-BuI	−0.796	−0.930	2.89	0.631	0.720	2.28	1.61	0.43	2.56	4.00
t-BuI	−0.776	−0.910	2.91	0.628	0.715	2.15	1.63	0.42	2.53	4.00
n-BuBr	−1.109	−1.230	2.73	0.656	0.760	3.00	1.69	0.41	2.35	3.80
sec-BuBr	−1.089	−1.210	2.73	0.656	0.760	2.99	1.56	0.44	2.38	3.80
t-BuBr	−0.879	−1.000	2.75	0.653	0.754	2.82	1.43	0.48	2.42	3.80
n-BuCl	−1.257	−1.369	2.63	0.674		3.50	1.49	0.46	2.22	3.65
sec-BuCl	−1.258	−1.370	2.64	0.672		3.45	1.46	0.47	2.24	3.65
t-BuCl	−1.138	−1.250	2.66	0.668		3.42	1.28	0.54	2.30	3.65

[a] In V vs SCE, ΔG°_4: standard Gibbs free energy (in eV) of the reaction $RXg + R^{\cdot DMF} \rightleftarrows RX^{DMF} + R^\cdot g$. [b] Estimated as in ref 5c, 17a, 17b. [c] Radius of the equivalent sphere. [d] Homogeneous and heterogeneous solvent reorganization factors (see text). [e] Dissociation energy of the C-X bond from thermochemical data in ref 18. [f] $\beta = v_0(2\pi 2\mu/D_{RX})^{1/2}$, v_0: C-X stretching vibration frequency (from ref 19a), μ: reduced mass of the C and X fragments. [g] Elongation of the C-X bond in the transition state at zero driving force from $y^\ddagger = \ln 2/\beta$ (see text). [h] In the transition state, from *g* and ref 19b. [i] In the van der Waals complex, from ref 19c, assuming that the van der Waals thickness of R· is approximately equal to that of a benzene ring.

Table II. Electrochemical Reduction of Butyl Iodides and Bromides in DMF. Comparison of the Experimental Data[a] with the Predictions of the Models

	experimental			theoretical					
compd	E_m at 0.1 V·s^{-1} (V vs SCE)	$\Delta G^\ddagger_{el}$ (eV)	α	$E^\circ_{RX/R\cdot+X^-}$ (V vs SCE)	$\Delta G^\ddagger_{el}$[b] (eV)	α[b]	$E^\circ_{RX/R\cdot+X^-}$ (V vs SCE)	$\Delta G^\ddagger_{el}$[c] (eV)	α[c]
n-BuI	−2.252	0.353	0.30	−1.075	0.376 (0.392)	0.34 (0.34)	−1.209	0.423 (0.380)	0.36 (0.35)
sec-BuI	−1.982	0.339	0.33	−0.796	0.312 (0.325)	0.32 (0.33)	−0.930	0.356 (0.317)	0.34 (0.34)
t-BuI	−1.839	0.340	0.32	−0.776	0.323 (0.337)	0.34 (0.34)	−0.910	0.370 (0.334)	0.36 (0.35)
n-BuBr	−2.756	0.359	0.25	−1.109	0.331 (0.312)	0.30 (0.29)	−1.230	0.368 (0.310)	0.31 (0.30)
sec-BuBr	−2.540	0.347	0.25	−1.089	0.390 (0.370)	0.32 (0.32)	−1.210	0.430 (0.369)	0.34 (0.33)
t-BuBr	−2.397	0.349	0.20	−0.879	0.332 (0.314)	0.30 (0.30)		0.370 (0.314)	0.32 (0.31)

[a] Temperature, 10 °C. [b] Values for $\gamma = 0$ and, between parentheses, for $\gamma = -0.008$ for BuI and $\gamma = 0.004$ for BuBr. [c] Values for $\gamma = 0$ and, between parentheses, for $\gamma = 0.037$ for BuI and $\gamma = 0.046$ for BuBr.

D_{RX} and from the C-X stretching frequencies.[18a] The values of the elongation of the C-X bond from its equilibrium position at the transition state for a zero driving force ensure (Figure 1).

$$y^\ddagger = \ln 2/\beta$$

It is seen that the length of the C-X bond in the transition state is much shorter than the C-X distance in the $R^\cdot + X^-$ van der Waals complex. This is even true for positive values of the driving force such as those involved in the electrochemical and homogeneous experiments.

An estimation of the radius of the sphere equivalent to each butyl halide is required for the determination of the homogeneous collision frequency, Z^{sol}, and for that of the homogeneous and heterogeneous solvent reorganization factors, λ_0^{hom} and λ_0^{het}. Since, at the transition state, the C-X bond elongation is small, a reasonable estimate is obtained as the half-sum of the RX and X^- radii. The first of these was obtained from $(3M/4\pi N_A\rho)^{1/3}$, M being the molar mass, ρ the density, and N_A the Avogadro number. The resulting values of the equivalent radius, a_1, are listed in Table I.

The solvent reorganization factors were derived from previous determinations of the electron transfer activation free energies in a large series of aromatic molecules in the same solvent, DMF.[3b] With these molecules there is little doubt that reorganization involves practically only the solvent. From the results described in ref 3b, it is apparent that, for isotopic homogeneous electron exchanges, the solvent reorganization factor varies as the inverse of the radius as predicted by Marcus theory[16a] but is less by a factor of ca. 1.6 than predicted by the theory. This can be explained by the fact that Marcus theory, being based on the Born model of solvation, overestimates the solvation free energies. For estimating our cross-exchange solvent reorganization factor we therefore used the Marcus relationship multiplying the radii by a factor of 1.6. The values listed in Table I ensued. Similarly, the experimental values obtained for the heterogeneous solvent reorganization factors in the same series of compounds were used to derive its values in the present case (Table I).

The homogeneous collision frequency was derived from the Debye-Smoluchovski equation

$$Z^{sol} = \frac{4.6310^{10}(a_1 + a_2)^2}{\mu} \qquad (9)$$

(Z^{sol} is expressed in $M^{-1}\cdot s^{-1}$; a_1 and a_2, the radii of the reactants, in Å; and μ, their reduced mass, in g). For the whole series of homogeneous mediators (Table III) Z^{sol} was found equal to 3×10^{11} $M^{-1}\cdot s^{-1}$ with a maximal deviation of ±10%, i.e., perfectly negligible in testing the models. The heterogeneous collision frequency ($Z^{sol} = (kT/2\pi m)^{1/2}$) was 4.6×10^3 and 5.2×10^3 $cm\cdot s^{-1}$ for the butyl iodides and butyl bromides, respectively.

The treatment of the electrochemical data was then as follows. At a given sweep rate, the transfer coefficient, α, can be considered as approximately constant along the cyclic voltammetric wave between the half-peak potential, $E_{p/2}$, and the peak potential, E_p, and to have as an average value its value at the potential $E_m = (E_{p/2} + E_p)/2$. Thus, as shown in the Appendix, the activation free energy of the forward electron transfer at the potential E_m is

$$\Delta G^\ddagger_{el} = \frac{RT}{F} \ln \frac{Z^{el}}{\left(\frac{\alpha F v D}{RT}\right)^{1/2}} - 0.145\frac{RT}{F} \qquad (10)$$

Table III. Homogeneous Reduction of Butyl Halides by Aromatic Anion Radicals in DMF. Comparison of the Experimental Data[a] with the Predictions of the Models[b]

			experimental		theoretical			
compd	mediator	d	E°_A	$\Delta G^\ddagger_{hom}$	$E^\circ_{RX/R\cdot+X^-}$	$\Delta G^\ddagger_{hom}$[e]	$E^\circ_{RX/R\cdot+X^-}$	$\Delta G^\ddagger_{hom}$[f]
n-BuI[c]	anthracene	1	−1.875	0.322	−1.075	0.448 (0.465)	−1.209	0.500 (0.455)
	9,10-diphenylanthracene	2	−1.800	0.355		0.477 (0.494)		0.530 (0.485)
	fluoranthene	3	−1.715	0.420		0.510 (0.527)		0.565 (0.519)
	perylene	4	−1.600	0.478		0.577 (0.575)		0.614 (0.568)
	benzo[*c*]chinoline	5	−1.440	0.562		0.626 (0.644)		0.687 (0.640)
sec-BuI	9,10-diphenylanthracene	1	−1.840	0.339	−0.796	0.299 (0.313)	−0.930	0.344 (0.306)
	naphthonitrile	2	−1.810	0.350		0.309 (0.323)		0.354 (0.316)
	4-cyanopyridine	3	−1.730	0.395		0.336 (0.350)		0.383 (0.344)
	phthalonitrile	4	−1.590	0.444		0.385 (0.400)		0.435 (0.395)
	terephthalonitrile	5	−1.510	0.504		0.415 (0.429)		0.467 (0.426)
	p-diacetylbenzene	6	−1.420	0.539		0.449 (0.464)		0.503 (0.462)
t-BuI	4-cyanopyridine	1	−1.730	0.345	−0.776	0.299 (0.313)	−0.910	0.345 (0.309)
	phthalonitrile	2	−1.590	0.392		0.347 (0.361)		0.396 (0.359)
	terephthalonitrile	3	−1.510	0.422		0.376 (0.390)		0.427 (0.389)
	p-diacetylbenzene	4	−1.420	0.455		0.410 (0.424)		0.463 (0.425)
	2-nitro-*o*-xylol	5	−1.350	0.477		0.437 (0.452)		0.492 (0.453)
	3-nitro-*o*-xylol	6	−1.240	0.526		0.482 (0.496)		0.540 (0.500)
n-BuBr[c]	m-toluonitrile	1	−2.270	0.336	−1.109	0.426 (0.405)	−1.230	0.468 (0.405)
	benzonitrile	2	−2.240	0.343		0.436 (0.416)		0.479 (0.415)
	methylbenzoate	3	−2.170	0.381		0.460 (0.440)		0.504 (0.440)
	benzo[*h*]chinoline	4	−2.120	0.394		0.478 (0.458)		0.523 (0.458)
	phenanthridine	5	−2.000	0.468		0.523 (0.502)		0.570 (0.504)
	anthracene	6	−1.875	0.523		0.571 (0.550)		0.620 (0.553)
sec-BuBr	phenanthrene	1	−2.420	0.272	−1.089	0.390 (0.371)	−1.210	0.430 (0.369)
	p-toluonitrile	2	−2.380	0.297		0.403 (0.383)		0.443 (0.382)
	benzonitrile	3	−2.260	0.346		0.443 (0.423)		0.486 (0.425)
	methylbenzoate	4	−2.190	0.367		0.468 (0.447)		0.512 (0.448)
	phenanthridine	5	−2.030	0.450		0.520 (0.505)		0.572 (0.507)
	anthracene	6	−1.900	0.490		0.576 (0.554)		0.624 (0.558)
	naphthonitrile	7	−1.810	0.512		0.612 (0.590)		0.662 (0.594)
t-BuBr	benzonitrile	1	−2.260	0.336	−0.879	0.315 (0.297)	−1.000	0.352 (0.295)
	methylbenzoate	2	−2.190	0.369		0.336 (0.318)		0.375 (0.319)
	phenanthridine	3	−2.030	0.412		0.388 (0.369)		0.430 (0.371)
	9,10-dimethylanthracene	4	−1.930	0.458		0.422 (0.403)		0.466 (0.406)
	anthracene	5	−1.900	0.466		0.433 (0.413)		0.477 (0.416)
	9,10-diphenylanthracene	6	−1.840	0.499		0.454 (0.435)		0.499 (0.438)
	4-cyanopyridine	7	−1.730	0.537		0.495 (0.475)		0.542 (0.480)
n-BuCl[c]	diphenyl	1	−2.540	0.477	−1.257	0.500 (0.482)	−1.369	0.540 (0.461)
	p-toluonitrile	2	−2.340	0.524		0.572 (0.553)		0.615 (0.532)
	m-toluonitrile	3	−2.270	0.548		0.598 (0.579)		0.641 (0.559)
	benzonitrile	4	−2.240	0.553		0.610 (0.590)		0.653 (0.571)
	methylbenzoate	5	−2.170	0.588		0.637 (0.617)		0.689 (0.598)
sec-BuCl	triphenylphosphine	1	−2.670	0.397	−1.258	0.445 (0.427)	−1.370	0.483 (0.407)
	diphenyl	2	−2.540	0.460		0.489 (0.470)		0.529 (0.450)
	phenanthrene	3	−2.420	0.482		0.531 (0.512)		0.572 (0.493)
	p-toluonitrile	4	−2.380	0.484		0.546 (0.527)		0.587 (0.507)
	benzonitrile	5	−2.260	0.556		0.590 (0.571)		0.634 (0.552)
t-BuCl	triphenylphosphine	1	−2.670	0.400	−1.138	0.400 (0.382)	−1.250	0.435 (0.362)
	diphenyl	2	−2.540	0.432		0.441 (0.423)		0.479 (0.403)
	phenanthrene	3	−2.420	0.478		0.482 (0.463)		0.521 (0.443)
	benzonitrile	4	−2.260	0.544		0.538 (0.519)		0.579 (0.500)

[a] Temperature, 10 °C unless otherwise stated. [b] All standard potentials in V vs SCE, all free energies in eV. [c] Temperature, 20 °C. [d] Conventional numbering of the mediators in Figure 2. [e] Values for $\gamma = 0$ and, between parentheses, for $\gamma = -0.008$ (BuI), 0.004 (BuBr), 0.023 (BuCl). [f] Values for $\gamma = 0$ and, between parentheses, for $\gamma = 0.037$ (BuI), 0.046 (BuBr), 0.048 (BuCl).

(v is the sweep rate and D the diffusion coefficient) and the transfer coefficient

$$\alpha = \frac{1.85}{E_{p/2} - E_p}\frac{RT}{F} \qquad (11)$$

The experimental values thus obtained are then compared with the values predicted on the basis of the first model ($\gamma = 0$), i.e., from eq 1

$$\Delta G^\ddagger_{el} = \frac{D_{RX} + \lambda_0^{het}}{4}\left[1 + \frac{E_m - E^\circ_{RX/R\cdot+X^-} - \Phi_r}{D_{RX} + \lambda_0^{het}}\right]^2$$

(Φ_r is the potential at the reaction site. We assumed that it is close to its value on a mercury electrode, i.e., in the electrode potential range of interest, $\Phi_r = -0.120$ V[2])

$$\alpha = \frac{1}{2}\left(1 + \frac{E_m - E^\circ_{RX/R\cdot+X^-} - \Phi_r}{D_{RX} + \lambda_0^{het}}\right)$$

The comparison between the experimental data and the prediction of the simple model ($\gamma = 0$) are shown in Table II for the two series of estimation of the $RX/R^\cdot + X^-$ standard potentials.

A similar comparison was made for the homogeneous kinetics of the reduction of the butyl halides by a series of aromatic anion

Table IV. Reduction of Butyl Halides in DMF. Estimation of the Empirical Factor γ for the Kinetic Model Involving a $R^{\cdot} + X^{-}$ Repulsive Term

				Y				
compd	$E^{\circ}_{RX/R\cdot+X^-}$	homog. red.	electrochem. red.	average	$E^{\circ}_{RX/R\cdot+X^-}$	homog. red.	electrochem. red.	av
n-BuI	−1.075	0.088	0.021		−1.209	0.128	0.052	
sec-BuI	−0.796	−0.061	−0.030	−0.008	−0.930	−0.009	0.019	0.037
t-BuI	−0.776	−0.006	−0.019		−0.910	−0.001	0.032	
n-BuBr	−1.109	0.060	−0.023		−1.230	0.092	0.007	
sec-BuBr	−1.089	−0.057	0.034	0.004	−1.210	0.086	0.063	0.046
t-BuBr	−0.879	−0.026	−0.014		−1.000	0.007	0.019	
n-BuCl	−1.257	0.040			−1.369	0.064		
sec-BuCl	−1.258	0.028		0.023	−1.370	0.053		0.048
t-BuCl	−1.138	0.001			−1.250	0.026		

Table V. Homogeneous and Electrochemical Reduction of Butyl Halides in DMF, Standard Deviations[a] of Activation Free Energies between the Predictions of the Two Models and the Experimental Data

	$E^{\circ}_{RX/R+X^-}$ with $\Delta G^{\circ}_4 = 0$[b]						$E^{\circ}_{RX/R\cdot+X^-}$ with $\Delta G^{\circ}_4 \neq 0$[b]					
	simple model ($\gamma = 0$)			modified model ($\gamma \neq 0$)			simple model ($\gamma = 0$)			modified model ($\gamma \neq 0$)		
compd	ϵ_{hom}	ϵ_{el}	ϵ_{hom+el}	ϵ_{hom}	ϵ_{el}	ϵ_{hom+el}	ϵ_{hom}	ϵ_{el}	ϵ_{hom+el}	ϵ_{hom}	ϵ_{el}	ϵ_{hom+el}
n-BuI	115	23	87	116	39	107	140	70	130	108	27	99
sec-BuI	66	27	62	53	14	49	22	17	21	57	22	53
t-BuI	48	17	45	30	3	28	9	30	14	31	6	28
global	71	23	66	73	24	68	78	45	73	70	20	65
n-BuBr	81	28	75	57	47	56	121	9	111	57	49	56
sec-BuBr	99	43	93	72	43	69	143	83	137	73	22	68
t-BuBr	34	27	33	52	35	50	11	21	13	51	35	49
global	74	33	70	61	42	59	107	49	101	61	37	58
n-BuCl	47		47	28		28	89		89	13		13
sec-BuCl	41		41	28		28	86		6	13		13
t-BuCl	6		6	32		32	40		40	39		39
global	37		37	29		29	77		77	23		23
total	65	27	62	59	34	57	90	57	87	57	30	55

[a] $\epsilon = [(\Delta G^{\ddagger}_{theor} - \Delta G^{\ddagger}_{expt})^2/N]^{1/2}$ (N = number of data points) in MeV. [b] See text and Table I.

radicals. The experimental value of the activation free energy, $\Delta G^{\ddagger}_{hom}$, is derived from the values of the rate constant, k_1, as

$$\Delta G^{\ddagger}_{hom} = \frac{RT}{F} \ln\left(\frac{Z^{sol}}{k_1}\right)$$

whereas the theoretical prediction for the simple model ($\gamma = 0$) is

$$\Delta G^{\ddagger}_{hom} = \frac{D_{RX} + \gamma_0^{hom}}{4}\left(1 + \frac{E^{\circ}_A - E^{\circ}_{RX/R\cdot+X^-}}{D_{RX} + \lambda_0^{hom}}\right)^2$$

where E°_A is the standard potential of the mediator couple. The results are shown in Table III.

For testing the more complicated model, in which the attractive part of the $R^{\cdot} + X^{-}$ potential energy curve is not neglected ($\gamma \neq 0$), we proceeded as follows.

In the electrochemical case, the predictions are now (from eq 8)

$$\Delta G^{\ddagger}_{el} = \frac{1}{4}[(1-\gamma)^2 D_{RX} + \lambda_0^{het}]\left[1 + \frac{E_m - E^{\circ}_{RX/R\cdot+X^-} - \Phi_r}{(1-\gamma)^2 D_{RX} + \lambda_0^{het}}\right]^2$$

and

$$\alpha = \frac{1}{2}\left[1 + \frac{E_m - E^{\circ} - \Phi_r}{(1-\gamma)^2 D_{RX} + \lambda_0^{het}}\right]$$

For the homogeneous case, $\Delta G^{\ddagger}_{hom}$ is simply derived from eq 1 and 8 in which λ_0 is replaced by λ_0^{hom} and ΔG° by $E^{\circ}_A - E^{\circ}_{RX/R\cdot+X^-}$. γ was iteratively adjusted to make the theroetical and experimental values of $\Delta G^{\ddagger}$ agree. In the electrochemical case, the kinetic data for a sweep rate of 0.1 $V \cdot s^{-1}$ were used in this purpose. In the homogeneous case, the fitting was carried out with a smoothed value of $\Delta G^{\ddagger}$ located in the center of the mediator standard potential range. The values of γ listed in Table IV ensued. Since no definite trend appears in the *n*-, *sec*-, *t*-Bu series for the same halogen, whereas the kinetics are clearly different when passing from one halogen to the other, we reprocessed the kinetic data according to the second model using for γ the average values indicated in Table IV. The results of the comparison between experimental data and theoretical predictions obtained in this way appear in Tables II and III (figures between parentheses).

To get a better view of the fitting between theory and experimental data, the comparison is shown graphically in Figure 2. It is seen that there is a satisfactory agreement between the experimental data and the predictions of both models. We also note that the more complicated model ($\gamma \neq 0$) does not improve significantly the matching of experimental data with theory. The degree of agreement between theory and experimental data is indicated in a more quantitative way in Table V under the form of standard deviations. On the whole population of butyl halides and of homogeneous and electrochemical experiments, the standard deviation is less than 90 meV. This is quite satisfactory in view of the experimental errors and also the uncertainty on the determination of the various quantities required to test the models. For example, the accuracy on thermochemical data leading to the estimation of the standard potentials and bond dissociation energies is not much better than 90 meV. We again see that the model with $\gamma \neq 0$ does not bring about a significant improvement vis-à-vis the simple model ($\gamma = 0$).

We noted earlier[5d] the variations in kinetics and thermodynamics when passing from one isomer of a butyl halide to another are small which also follows from the theoretical model. Very substantial differences are found when passing from one halogen

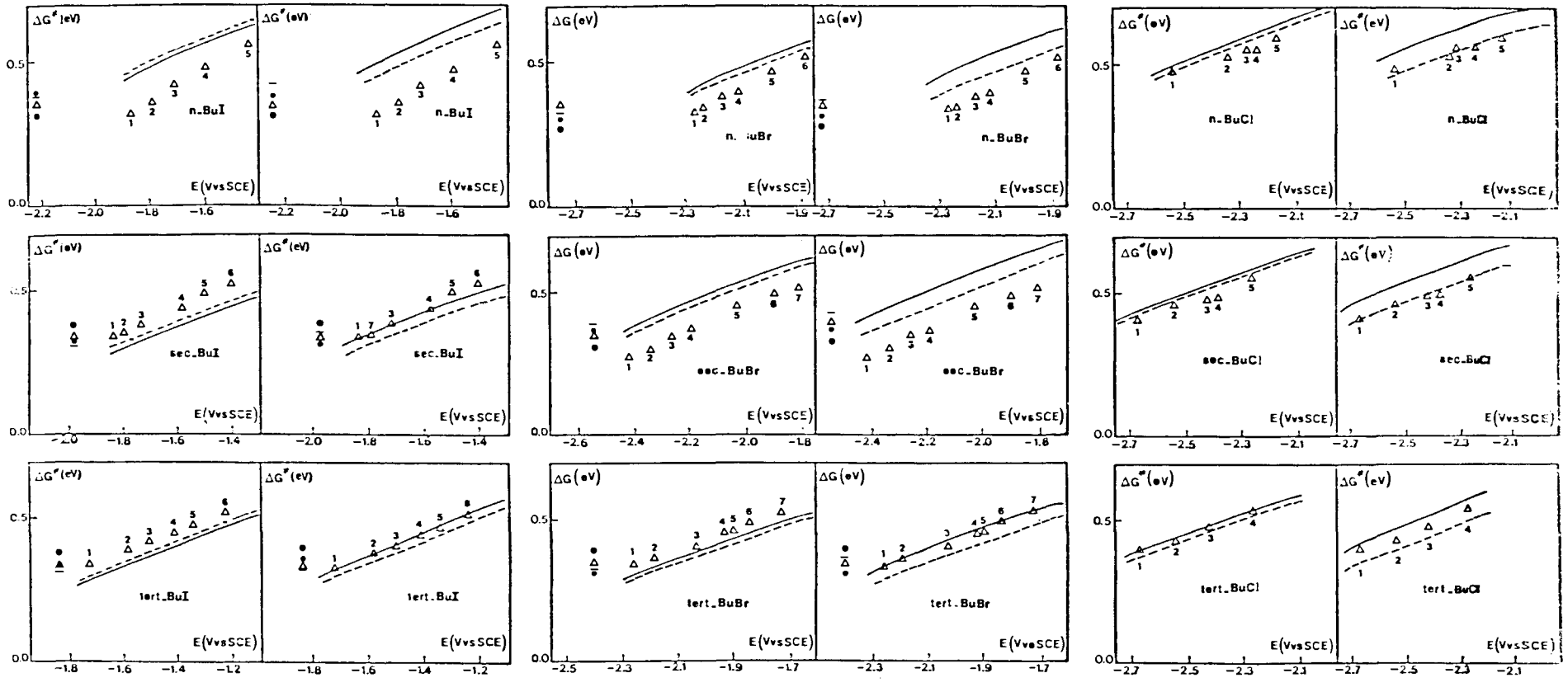

Figure 2. Electrochemical and homogeneous reduction of butyl halides in DMF. Comparison between the two models and the experimental data. The left-hand-side and right-hand-side diagrams correspond to an estimation of $E°_{RX/R^{\bullet}+X^{-}}$ in which $\Delta G°_4 = 0$ and $\Delta G°_4 \neq 0$, respectively (see Table I). The points given by Δ represent the experimental data (e, electrochemical; 1, 2, 3, ..., homogeneous data numbered as indicated in Table III). Solid line, simple model ($\gamma = 0$); dashed line, model with an attractive term in the $R^{\bullet} + X^{-}$ potential energy curve ($\gamma \neq 0$) for the homogeneous reactions; ●, simple model ($\gamma = 0$); –, model with $\gamma \neq 0$ in the electrochemical case.

to the other in good agreement with the proposed model.

As discussed in detail elsewhere,[4c] another system giving a satisfactory agreement between experimental data and the predictions of the simple model is the electrochemical and homogeneous reduction of *trans*-1,2-dibromocyclohexane.

Conclusions

A very simple model of dissociative electron transfer has been developed. Based on a Morse curve description of the potential energy surfaces for bond breaking, it leads, for homogeneous and heterogeneous processes, to a quadratic activation–driving force free energy relationship with the standard activation free energy being the sum of two contributions characterizing bond breaking and solvent re-organization, respectively. The latter can be estimated on the basis of the Marcus dielectric continuum model for solvation. The former appears as equal to one-fourth of the bond dissociation energy.

Application of the model to the kinetics of homogeneous and electrochemical dissociative electron transfer to alkyl halides leads to a satisfactory agreement between experimental data and theory. The contribution of bond breaking to the standard activation energy is typically 80% of the total, the remaining 20% dealing with solvent re-organization.

Acknowledgment. C.P. Andrieux (Université de Paris 7), R.A. Marcus (Caltech, Pasadena), and P. Millié (CEA, Saclay) are gratefully thanked for helpful discussions during the preliminary stages of this work.

Appendix

Derivation of Equations 1, 4, and 5. At the transition state

$$D_{RX}[1 - 2\exp(-\beta y^{\ddagger})] + \frac{\kappa}{2}[(x^{\ddagger} - x_1)^2] = \Delta G^{\circ}$$

The activation free energies are expressed as

$$\Delta G_1^{\ddagger} = D_{RX}[1 + \exp(-2\beta y^{\ddagger}) - 2\exp(-\beta y^{\ddagger})] + \frac{\kappa}{2}(x^{\ddagger} - x_1)^2$$

$$\Delta G_{-1}^{\ddagger} = D_{RX}\exp(-2\beta y^{\ddagger}) + \frac{\kappa}{2}(x^{\ddagger} - x_2)^2$$

Minimizing the activation free energies leads to

$$\kappa(x^{\ddagger} - x_1)\,dx^{\ddagger} + D_{RX}[-2\beta\exp(-2\beta y^{\ddagger}) + 2\beta\exp(-\beta y^{\ddagger})]\,dy^{\ddagger} = 0$$

$$\kappa(x^{\ddagger} - x_2)\,dx^{\ddagger} - D_{RX}2\beta\exp(-2\beta y^{\ddagger})\,dy^{\ddagger} = 0$$

Thus

$$\frac{x^{\ddagger} - x_1}{1 - \exp(\beta y^{\ddagger})} = \frac{x^{\ddagger} - x_2}{1} = (x_1 - x_2)\exp(-\beta y^{\ddagger})$$

and

$$x^{\ddagger} - x_1 = (x_1 - x_2)[\exp(-\beta y^{\ddagger}) - 1]$$

$$x^{\ddagger} - x_2 = (x_1 - x_2)\exp(-\beta y^{\ddagger})$$

It follows that

$$(D_{RX} + \lambda_0)[1 - 2\exp(-\beta y^{\ddagger})] = \Delta G^{\circ}$$

with

$$\lambda_0 = \frac{\kappa}{2}(x_1 - x_2)^2$$

and thus

$$\exp(-\beta y^{\ddagger}) = \frac{1}{2}\left(1 - \frac{\Delta G^{\circ}}{D_{RX} + \lambda_0}\right)$$

Equations 1 and 4 ensue with

$$\Delta G_0^{\ddagger} = \frac{D_{RX} + \lambda_0}{4}$$

Derivation of Equation 8. Starting now from eq 6 and 7, at the transition state

$$D_{RX}[(1 - \gamma^2) - 2(1 - \gamma)\exp(-\beta y^{\ddagger})] + \frac{\kappa}{2}[(x^{\ddagger} - x_1)^2 - (x^{\ddagger} - x_2)^2] = \Delta G^{\circ}$$

with

$$\Delta G_1^{\ddagger} = D_{RX}[1 - \exp(-y^{\ddagger})]^2 + \frac{\kappa}{2}(x^{\ddagger} - x_1)^2$$

$$\Delta G_{-1}^{\ddagger} = D_{RX}[\gamma - \exp(-y^{\ddagger})]^2 + \frac{\kappa}{2}(x^{\ddagger} - x_2)^2$$

Minimizing the activation free energies leads to

$$\frac{x^{\ddagger} - x_1}{1 - \exp(\beta y^{\ddagger})} = \frac{x^{\ddagger} - x_2}{1 + \gamma\exp(\beta y^{\ddagger})} = \frac{(x_1 - x_2)\exp(-\beta y^{\ddagger})}{1 - \gamma}$$

and thus to

$$x^{\ddagger} - x_1 = \frac{\exp(-\beta y^{\ddagger}) - 1}{1 - \gamma}(x_1 - x_2)$$

$$x^{\ddagger} - x_2 = \frac{\exp(-\beta y^{\ddagger}) - \gamma}{1 - \gamma}(x_1 - x_2)$$

Hence

$$\exp(-\beta y^{\ddagger}) = \frac{1}{2(1 - \gamma)}\left[1 - \gamma^2 - \frac{\Delta G^{\circ}}{D_{RX} + \frac{\lambda_0}{(1 - \gamma)^2}}\right]$$

Equation 8 ensues.

Derivation of Equations 10 and 11. Let $\Delta G^{\ddagger}_{el}$ designates the activation free energy at the potential E_m, mid-way between the half-peak and peak potentials, $E_{p/2}$ and E_p

$$\frac{i}{FS} = Z^{el}\exp\left[\left(-\frac{F}{RT}\right)(\Delta G^{\ddagger} + \alpha\Delta E)\right] = k\exp\left(-\frac{\alpha F}{RT}\Delta E\right)$$

with

$$k = Z^{el}\exp\left(-\frac{F}{RT}\Delta G^{\ddagger}\right)$$

assuming that the transfer coefficient does not vary appreciably between $E_{p/2}$ and E_p and has the value, α, it has for $E = E_m$ (i is the current flowing through the electrode and S is the electrode surface area). Thus introducing the dimensionless current and potential variables

$$\Psi = \frac{i}{FSC^{\circ}D^{1/2}(\alpha Fv/RT)^{1/2}}$$

$$\xi^{*} = -\frac{F}{RT}(E - E^{\circ}) + \ln\frac{k}{D^{1/2}(\alpha Fv/RT)^{1/2}}$$

(C°, concentration of the substrate; D, diffusion coefficient, v, sweep rate; E, electrode potential; E°, standard potential), it follows that the peak characteristics are such that[20]

$$\xi^{*}_p = 0.78 \qquad \xi^{*}_p - \xi^{*}_{p/2} = 1.85$$

Thus

$$\Delta G^{\ddagger} = \frac{RT}{F}\ln\left[\frac{Z^{el}}{\left(\frac{\alpha FvD}{RT}\right)^{1/2}}\right] - 0.145\frac{RT}{F} \qquad (10)$$

$$\alpha = \frac{RT}{F}\frac{1.85}{E_{p/2} - E_p} \qquad (11)$$

Registry No. *n*-BuI, 542-69-8; *sec*-BuI, 513-48-4; BuI, 558-17-8; *n*-BuBr, 109-65-9; *sec*-BuBr, 78-76-2; BuBr, 507-19-7.

(20) (a) Matsuda, H.; Ayabe, Y. *Z. Elektrochem.* **1955**, *59*, 494. (b) Nadjo, L.; Savéant, J. M. *J. Electroanal. Chem.* **1973**, *44*, 327.